Lateral distribution of muon pairs in deep underground muon showers*

G. H. Lowe,† H. E. Bergeson, J. W. Keuffel,‡ M. O. Larson,‖ J. L. Morrison, and W. J. West
University of Utah, Salt Lake City, Utah 84112

(Received 13 October 1975; revised manuscript received 12 December 1975)

The lateral distribution of muon showers deep underground in the Utah muon detector has been studied. The results are presented in the form of a decoherence curve, which is defined to be the rate of pairs of coincident muons in two small detectors (as a function of their separation) divided by the product of the areas of the detectors. Rates are measured for separations from 1 to greater than 60 m for depths ranging from 2.4×10^5 g cm^{-2} to 5.6×10^5 g cm^{-2} and zenith angles ranging from 42.5 to 62.5 degrees. Significant improvements on previously reported data have been made due to increased detector-memory size, improved triggering efficiency, longer running time and better statistical analysis. When the decoherence curve is parameterized by the function $R(x) = R_0 e^{-x/x_0}$ the value of the mean separation x_0 at 47.5°, 2.4×10^5 g cm^{-2} is 11.21 ± 0.38 m. In a modified scaling model this separation suggests an average transverse momentum of roughly 0.65 GeV/c for muons from hadron-air collisions with energy > 10 TeV.

I. INTRODUCTION

Multiple muons observed deep underground offer a unique peek at the properties of the hadronic interaction at energies up to 10^{15} eV. The recent theoretical developments of scaling and limiting fragmentation make it possible to extend predictions, in a reasonably unambiguous way, from the measurements made at accelerators at up to 10^{12} eV. The multiple-muon predictions depend upon the spectrum and composition of the primary cosmic rays as well as the collision mode.

The schematic diagram shown in Fig. 1 gives an indication of how muons observed deep underground may be used to study the properties of the primary spectrum and interactions of the incoming primary cosmic rays. A hadronic cascade is initiated by a primary nucleus at an average depth of 80 g cm^{-2} in the atmosphere. Pions and kaons in the cascade may decay to produce muons; the average decay probability for the pions is $P_D \sim (90\ \mathrm{GeV}/E_\pi)\sec\theta$, where θ is the zenith angle of the particle trajectory. In the interactions which produce the cascade some transverse momenta p_T is imparted to the secondary particles. Since the rock in the mountains above the Utah muon detector acts as an energy analyzer the separation of a muon from the shower core can be expected to give an estimate of the p_T of the interactions which produced the muon. To a first approximation one might expect the separation from the shower core to be given by $d = (p_T/E_\mu)h\sec\theta$, where h is the height of production. Thus, for typical values of $h\sec\theta = 20$ km, $E_N = 2000$ GeV, and $p_T = 0.5$ GeV/C, $d = 5$ m.

This paper describes the measurement of the lateral distribution of the muon showers studied in the Utah muon detector. The lateral distributions are flatter than the predictions[1] of a model with Feynman scaling applied to hadronic inter-

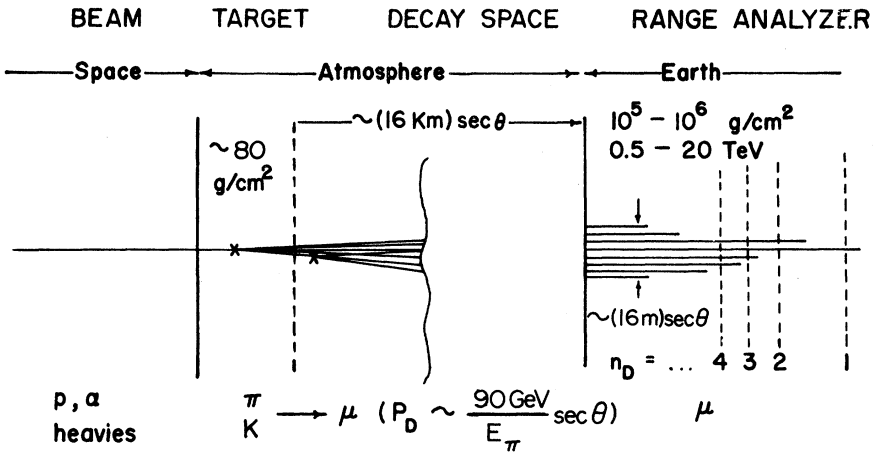

FIG. 1. Schematic drawing of the high-energy muon component of an energetic cosmic-ray event.

actions and the transverse momentum distribution of secondary mesons determined by accelerator measurements. An earlier paper[2] gave the measured rates of multiple muon events in fiducial planes of 80 m^2 and 100 m^2.

II. APPARATUS

The main detector has been described in some detail.[3-7] Briefly, it consists of 600 cylindrical spark counters arrayed in 15 vertical planes, each 6×10 m^2 as shown in Fig. 2. A trigger is provided by water-filled Cherenkov counters. The spark counters resemble oversized Geiger counters, 15 cm diam$\times$10 m long, but operated in a pulsed mode at a higher pressure so that the discharge is a sharply localized corona spike which is detected by means of a sonic ranging system. The location along the axis of the spark counter is known to within ±3 mm. Spark counters are sensitive to traversing ionizing particles for only 2 μsec after the time of the pulse. The detector is sufficiently thick that problems due to soft accompaniment are negligible. The angle between muon tracks in an event in the detector is on the average less than one degree, and no evidence of convergence or divergence of the tracks has been found.

Originally the detector had a ferrite-core memory system which was capable of storing information from as many as 108 sparks in the cylindrical spark counters for any given event. Since, on the average, each muon in the detector has associated with it 10 sparks, the ferrite-core memory severely limited the maximum observable multiplicity. Later the ferrite-core memory was replaced with a semiconductor shift register memory capable of storing information from 1000 sparks. These data were recorded on magnetic tapes which provide the basis for computer reconstruction and analysis of muon showers in the detector.

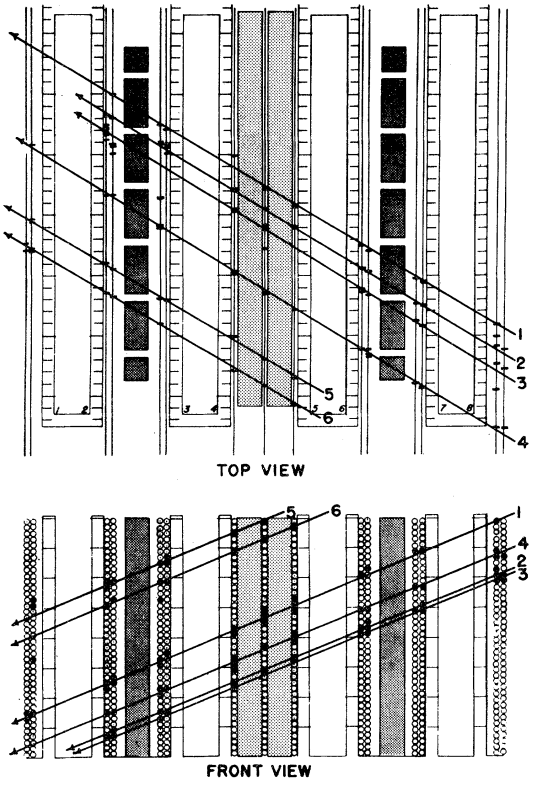

FIG. 2. A plot of an event which contains 6 muons in the main Utah detector. The three major components of the detector are: (1) Four directional Cherenkov tanks (whose walls are labeled 1–8 in the top view) which indicate the passage of left or right-going muons. (2) Fifteen stacks of 40 sonic ranging cylindrical spark counters which provide muon trajectory information. The coordinates of the sparks in the top view are obtained from the time delays of the acoustical pulses. (3) Two iron magnets (shaded) which determine the charge of the muon.

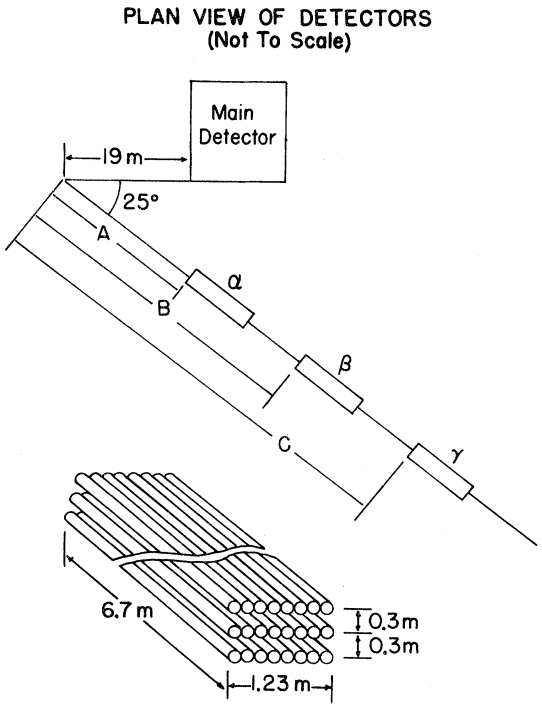

FIG. 3. The movable outrigger detectors α, β, and γ shown in a top view together with the main detector. Each outrigger consists of 3 planes of 8 cylindrical spark counters (bottom). The position of α was not changed during the experiment and had the value A = 24.9 m. The distances B and C were changed several times. The maximum value of C was 84.6 m.

In addition to the main detector, three outrigger detectors labeled α, β, γ in Fig. 3 are mounted on movable mine cars located in an adjacent tunnel. Each outrigger consists of 24 spark counters which are mounted in three horizontal planes with 8 counters per plane. The trigger for the outriggers is provided by the main detector. Because the spark-counter planes in the outrigger are more closely spaced than the planes in the main detector, the angular resolution of the outrigger can be as large as 20° in the worst direction with a more typical number being 10°.

III. ANALYSIS

Because of the very complex aperture and triggering requirements of the Utah detector it is necessary to devise a means to present the data in a manner independent of detector geometry. The means chosen is that of a decoherence curve (or pair rate as a function of separation) which was first described in a pioneering 1952 paper by Barrett *et al.*[8] The decoherence curve here is defined to be the coincident counting rate per second per steradian of two small detectors (as a function of their separation) divided by the product of the areas of the two small detectors. Earlier measurements[7-9] have shown that the decoherence curve can be characterized approximately by the form $R(x)=R_0e^{-x/x_0}$, where $x_0\simeq 10$ m at $\theta=45°$ and depth $=2.4\times10^5$ g cm^{-2}.

In order to trigger the detector muons must pass through at least two of the Cherenkov counters in the main detector. The number of small detectors at a given separation times the areas of the detectors (hereafter called a weight factor) is evaluated taking into account the triggering and muon recognition requirements of the detectors. For purposes of illustration consider that the weight factors are approximately the number of pairs of 1-m^2 detectors at a separation x which could together trigger the detectors at a given zenith and azimuth angle. In order to calculate the weight factors for the main detector, the solid angle is divided into 5° zenith angle (θ) by 10° azimuth angle (ϕ) segments, and the detector area is divided into 1-m^2 pieces. Pairs of area pieces are then selected such that muons passing through each area would traverse at least three spark-counter groups. Furthermore, the muons passing through the two selected areas must satisfy the Cherenkov triggering requirement of passing through the Cherenkov tanks within prescribed limits. These prescribed limits are chosen to ensure high triggering efficiency; each tank must have a muon within the pair of areas which traverses the back wall and at least one foot within the forward wall of the tank. The separation x between each pair of areas which satisfy the above requirements is calculated and the pairs are sorted into separation bins of width 1 m in the range 0 to 11 m. The weight factor at a given separation is then given approximately by the number of equivalent pairs of 1-m^2 detectors at that separation. In practice the detector is divided into smaller and smaller areas until the calculated weight factors converge to a limit.

The weight factors for the outrigger are calculated in the same manner taking into account that the outrigger trigger is provided by the main detector. Pairs of areas which contribute to the outrigger weight factors consist of one in the main detector and one in the outrigger. Thus, a muon which passes through the area being considered in the main detector must be capable of triggering the detector independently. The area in the outrigger must be such that a muon passing through it traverses all three rows of counters. The pairs of areas for the outrigger and main detector had possible separations ranging from 10 to 78 m varying according to the positions A, B, and C (see Fig. 3) of the outriggers on the track during different runs.

The data are analyzed in the following manner. When a shower of muons strikes the detectors, pairs of muons are selected such that the pair could have triggered the detectors and be recognized independently of any other muons (a muon must pass through three groups of counters for the main detector or three rows of counters for the outrigger). Event efficiency is determined from the measured Cherenkov efficiencies[2] taking into account all muons in the event. The separations between the muons in the accepted pairs are calculated and the pairs sorted into bins. The end result is the number of pairs counted during the live time in each x, θ, ϕ bin and the number of pairs corrected for event Cherenkov efficiency and individual muon-pair spark-counter efficiency. Division by the weight factor, solid angle, and run time at that x, θ, ϕ bin then results in a decoherence curve for that bin.

Since the number of pairs which contribute to the decoherence curve from an event which has n_D muons detected is $n_D(n_D-1)/2$, it is critically important that event-recognition efficiency be high for events of all multiplicities. Two different computerized pattern recognition programs were used for event detection for the main detector. One worked with events having smaller than 109 total sparks in the counters, and the second worked with events having greater than 108 sparks in the counters. The efficiency of both programs was measured for muons which met the aperture

requirement of passing through three groups of spark counters. The efficiency of the first program was indistinguishable from 100% and the second $(97 \pm 3)\%$ for all muons separated by a distance of greater than 0.3 m. It was found that 20% of the pairs come from events which have greater than 108 sparks. Therefore, only data taken after the change in the memory system (with a run time of 1.855×10^7 sec) could be used for the decoherence curve of pairs in the main detector.

Another program was used for outrigger event recognition. In order to be counted, an event in the outrigger must have satisfied the following criteria: (1) The track in the outrigger must be parallel to the tracks in the main detector to within the resolution of the detectors. (2) Only those tracks which have three or more collinear sparks, one in each plane of spark counters are accepted. All events having sparks in all three planes of one outrigger where a question existed as to the accuracy of the main-detector event-recognition analysis were hand scanned. The net efficiency of outrigger event recognition was indistinguishable from 100%.

It was found that events which have an outrigger muon meeting the above criteria tended to have small numbers of muons in the main detector. Therefore, data collected over the entire period with four different sets of outrigger positions could all be used in the analysis. The average total run time for each outrigger was 3.4×10^7 sec.

To determine the spurious background rate the outriggers were pulsed for the equivalent of 6×10^6 sec running time. No track was observed which could have satisfied even criterion 2 above.[7]

The triggering efficiency of the detector was measured in the following manner. For Cherenkov tanks, a muon was required to pass within prescribed boundaries on the inside of the tank and an independent trigger associated with a muon must have been produced by tanks other than the one being measured. Spark-counter efficiencies were measured by requiring that a trajectory be recognizable without the presence of the counter being measured. Extensive tests were made of the consistencies of the triggering logic.

The pair rates were corrected for the measured detector triggering efficiency. Earlier work[10] showed agreement within about 5% for measured muon intensities before and after the increase of single-muon over-all detection efficiency to ~85%. As more muons pass through the Cherenkov tanks in an event, more light is produced, and the triggering efficiency of the detector approaches 100%. The average double-muon event efficiency was 91% and showed no change with time. Single spark-counter efficiency averaged 90%. With the redundancy of spark counters, less than 4% of the single muons and fewer of the multiples were lost in the main detector. Outrigger counter efficiency, taking into account the requirement that all three rows of counters must fire, was 65%. As an over-all check on efficiency, the position of outrigger α was unchanged during the course of the experiment. It was found that the pair rates for the three blocks[2] of data used are consistent.

Rock depths for different $(\theta) - (\phi)$ bins were determined from 7.5-minute series topographical maps of the United States Geological Survey to an accuracy of 6 m.[11] These depths were converted into grams per square centimeter by multiplying by the rock density. Direct measurements of the density are limited in the number of points of access where samples may be taken, but an average of 2.61 was adopted by Keuffel *et al.*[12] Cassiday *et al.*[13] measured the vertical muon intensity at 10 locations along the access tunnel to the detector and by comparison with the world survey curve deduced a density of 2.55 ± 0.04. The Cassiday measurements surveyed the rock which corresponds to a slant depth around 2.4×10^5 g cm^{-2} for the detector. In order that the muon flux data fit a survey of the worth depth intensity curve[10,14] it was assumed that for depths less than 2.8×10^5 g cm^{-2} the density was 2.55 and for greater depths the density was 2.59. A Z^2/A correction has been made in order to convert the Utah rock which has a Z^2/A of 5.65 to standard rock which has a Z^2/A of 5.50.[15] Atmospheric depth traversed has been added to the rock depth (in grams per square centimeter) to give total depth.

Since the data are scattered over a wide range of depths, zenith angles, and separations, it is necessary to consolidate them in some way. If one knows the functional dependence of $R(x)$ on depth, angle, and separation to be given by some function $f(h, \theta, x)$, then the best value of $R(x)$ at some centered depth c is given from maximum likelihood as

$$R_c(x_c) = \frac{\sum N_i}{\sum \epsilon_i \omega_i \Delta\Omega_i \tau_i f(h_i, \theta_i, x_i)/f(h_c, \theta_c, x_c)}, \tag{1}$$

where N_i is the number of counts in the bin with angle θ_i, depth h_i, and separation x_i, ϵ_i is the triggering efficiency, ω_i the weight factor, $\Delta\Omega_i$ is the solid angle, and τ_i the run time for the bin. If a function f can be chosen that describes the data reasonably well, then by successively fitting the parameters of f, recentering the data, and iterating, the best values of $R_c(x_c)$ can be found.

If the final fits for f produce good values of χ^2 it can be assumed that the centering function is adequate. $R(x)$ has previously been found to fit the function $R(x)=R_0e^{-x/x_0}$. The form for the dependence of R_0 and x_0 on depth and angle must then be established.

As shown in Sec. I, x_0 is expected to be approximately proportional to $E_\mu^{-1}\sec\theta$. Adcock *et al.*[16] taking into account more detailed considerations predict that the form should be $x_1E_\mu^{-0.8}\sec^{1.3}\theta$. Thus, a good form to guess for x_0 is $x_0=x_1E_\mu^{\gamma}\sec^{\beta}\theta$.

The rate of inclusive doubles in 80 m^2 (inclusive here used in the same manner as in accelerator experiments) is given by

$$R(2\text{'s inclusive})=\sum_{n_D>1}\frac{n_D!J(n_D)}{2!(n_D-2)!}=\int\int_{80\,\mathrm{m}^2}\frac{R(x)}{2}\,dA_1dA_2\simeq\int\int_{80\,\mathrm{m}^2}\frac{R_0e^{-x/x_0}}{2}\,dA_1dA_2\,, \tag{2}$$

where x is the distance between two small detectors dA_1 and dA_2, n_D is the number of detected muons, and $J(n_D)$ is the rate of n_D muons in 80 m^2. It has been established[2] that the depth dependence of $J(n_D)$ for values of n_D from 1 to 5 is approximately the same. This depth dependence can be fit very well over the range of depths in question by an exponential which suggests a form for R_0, i.e., $R_0=R_1e^{-h/\lambda}$, where h is the depth and λ the falloff depth. However, the integral has dependence on x_0 which is a function of $\sec\theta$ and E_μ. (Note that E_μ can be approximately related to h by the range energy relationship described in earlier papers.[10,11,14] This suggests that a better form might be $R_0=R_1e^{-h/\lambda}\sec^{\alpha}\theta$. Adcock *et al.*[16] predict the form $R_0=R_1E_\mu^{-1.69}\sec^{-0.8}\theta$, which turns out to be similar to the chosen form over the depth and angular ranges fitted.

The method chosen is to initially let λ be large, x_1 large and $\alpha=\beta=\gamma=0$ (i.e., no centering). The values of $R_c(x)$ are then calculated for the centers of the bins. These data are then fit at seven depth-angle bins to the function $R(x)=R_0e^{-x/x_0}$ by a maximum-likelihood fit.[17] Poisson statistics are used since the number of counts in each separation bin is small for large separations. The errors on R_0 and x_0 turn out to be almost Gaussian. The separation bin from 0 to 1 m is not used because of inefficient recognition of muons which were closer together than 0.3 m in the Utah detector. The different values of R_0 and x_0 are then fit with a Gaussian fitting routine to obtain new values for R_1, λ, α, x_1, β, and γ. These values are then used to recenter the data, and the process is continued until the values of R_1, λ, α, x_1, β, and γ converge.

IV. RESULTS

The values obtained from the fits are (with h in g cm^{-2} and E_μ in GeV)

$$R_0\alpha(\sec\theta)^{-1.01\pm0.14}\exp[-h/(7.88\pm0.25)\times10^5]$$

with $\chi_r^2=1.08$

and

$$x_0=11.14\ \mathrm{m}\left(\frac{\sec\theta}{\sec47.5}\right)^{1.93\pm0.25}\left(\frac{E_\mu}{951}\right)^{-0.93\pm0.11}$$

with $\chi_r^2=0.84$.

For the form of R_0 predicted by Adcock *et al.*[16] the values obtained were

$$R_0\alpha(\sec\theta)^{-1.04\pm0.14}E_\mu^{-2.16\pm0.07}\ \text{with}\ \chi_r^2=2.19.$$

For the fits to R_0 and x_0 the error matrix showed rather large correlations between the coefficients of the angular dependence and the depth or energy. This correlation is due to the increase of depth with zenith angle owing to the nature of the terrain above the detector.

Table I lists the best values for R_0 and x_0 with errors obtained at each depth and angle for the various Poisson fits. The statistical errors in R_0 and x_0 are much larger than those produced by the centering function. Five sets of decoherence measurements and best fits are shown in Fig. 4. Upper limits on bins with 0 counts correspond to 1 count, and the remainder of the errors are pure Gaussian. All the indicated fits are done using Poisson statistics in order to account properly for the bins with small numbers of counts. Table I also indicates approximately the mean primary-proton energy necessary to produce a muon pair which will penetrate to this appropriate depth; higher energies are necessary if the muon multiplicity is greater than 2.

The plots and the size of χ^2 in the depth-angle bins with good statistics give an indication that the function R_0e^{-x/x_0} does not describe the decoherence curve to the accuracy of the statistics. A form that could fit better would have a flatter slope near the origin, a steeper slope for intermediate values of x, and a flatter slope for large values of x. From Adcock et al.[16] and our own calculations[1] the plots were expected to be somewhat concave, but the flattening at small separations is not yet understood. Extensive hand scanning of events revealed no systematic errors.

TABLE I. Values of R_0 and x_0 from fits. The values of χ^2 in the table were computed in the standard manner for separation bins having greater than 4 counts. The sum of the expected number of counts for all bins having less than 5 counts was compared to the sum of the actual number of counts in these bins in order to make the χ^2 contribution from them meaningful. Errors in the table are multiplied by $(\chi_r^2)^{1/2}$ for χ_r^2 greater than 1 in order to take into account systematic errors. For comparison to other data the percent error indicated under density should be added to the error in R_0 in order to take into account the variations in rock density above the Utah detector. E_0 is a rough estimate of the mean primary proton energy for production of a pair of muons penetrating to the given depth.

		Zenith angle (degrees)	Depth ($g\,cm^{-2}$)	R_0 ($m^{-4}sec^{-1}sr^{-1}$)	x_0 (m)	χ^2/points	Density error	E_0 (TeV)
1	Combined	47.5	2.4×10^5	$(1.72\pm0.03)\times10^{-6}$	11.21 ± 0.38	26.7/20	6%	100
	Main detector	(40–55)	$(2.0–2.8)\times10^5$	$(1.76\pm0.05)\times10^{-6}$	10.60 ± 0.65	18.6/10		
	Outriggers			$(1.75\pm0.34)\times10^{-6}$	11.46 ± 1.06	5.9/10		
2	Combined	47.5	3.2×10^5	$(6.29\pm0.23)\times10^{-7}$	6.89 ± 0.33	17.4/14	7%	160
	Main detector	(45–55)	$(2.8–3.6)\times10^5$	$(6.03\pm0.26)\times10^{-7}$	7.49 ± 0.55	4.5/10		
	Outriggers			$(4.37\pm2.65)\times10^{-7}$	7.24 ± 1.51	5.5/4		
3	Combined	62.5	3.2×10^5	$(4.35\pm0.17)\times10^{-7}$	14.91 ± 1.55	59.0/20	7%	160
	Main detector	(55–70)	$(2.8–3.6)\times10^5$	$(4.16\pm0.20)\times10^{-7}$	17.8 ± 3.4	19.7/10		
	Outriggers			$(3.1\pm1.5)\times10^{-7}$	17.1 ± 5.9	30.0/10		
4	Combined	62.5	4.0×10^5	$(1.45\pm0.08)\times10^{-7}$	10.04 ± 1.10	20.3/14	8%	270
	Main detector	(55–70)	$(3.6–4.4)\times10^5$	$(1.35\pm0.09)\times10^{-7}$	11.9 ± 2.0	11.3/10		
	Outriggers			$(1.2\pm1.0)\times10^{-7}$	9.9 ± 3.8	5.9/4		
5	Combined	62.5	4.8×10^5	$(6.73\pm0.82)\times10^{-8}$	7.9 ± 1.4	2.8/8	9%	470
	Main detector	(60–70)	$(4.4–5.2)\times10^5$	$(6.4\pm1.1)\times10^{-8}$	8.7 ± 2.8	3.4/8		
	Outriggers			$(2.6\pm5.3)\times10^{-7}$	5.0 ± 2.7	···		
6	Main detector [a]	72.5	4.0×10^5	$(1.31\pm0.35)\times10^{-7}$	11.0 ± 7.0	10.8/10	8%	270
		(70–80)	$(3.6–4.4)\times10^5$					
7	Combined	72.5	4.8×10^5	$(3.83\pm0.66)\times10^{-8}$	13.6 ± 6.4	5.7/9	9%	470
		(70–80)	$(4.4–5.2)\times10^5$					

[a] No outrigger weight factors for this bin.

Systematic differences between the outrigger and the main detector are checked by separate fits of the function R_0e^{-x/x_0} to the main detector and the outrigger data points. (See Table I.) For each of the 7 depth-angle bins the values of (R_0, x_0) for the main detector and the outrigger agree to within statistical accuracy. In turn, both are in agreement with fits to (R_0, x_0) for all the data. The outrigger fit at 10-m separation is above that for the main detector at 2.4×10^5 $g\,cm^{-2}$. For the next three points the outrigger fit at 10-m separation is below that for the main detector. This may be an indication of some systematic efficiency error (or an error as discussed in the previous paragraph in the form of the fitting function). However, when all the data are centered at 45° and 2.5×10^5 $g\,cm^{-2}$, there is no evidence for any discrepancy.

The fits of the functional dependence f of R_0 and x_0 used the errors as indicated in the table. As a test of the consistency of the centering function data from the ranges $(1.9–2.9)\times10^5$ $g\,cm^{-2}$, 35°–65° and $(2.9–3.9)\times10^5$ $g\,cm^{-2}$, 35°–65° were centered to the value 45°, 2.5×10^5 $g\,cm^{-2}$. Data from the two sets come from considerably different average zenith angles due to the zenith angle-depth correlation of the terrain above the detector. The two curves agree with each other extremely well.

V. COMPARISON WITH OTHER EXPERIMENTS

Earlier work[7,9] from Utah did not include the 20% contribution to the main-detector decoherence curve resulting from events which had greater than 108 sparks. As might be expected, the present work disagrees with that of Coats *et al.*[7] and Davis *et al.*[9] in the main detector. Agreement with the previous outrigger results of Coats *et al.* is excellent. The 20% change explains well the possible discrepancy between the main detector and the outrigger discussed by Coats *et al.*

The net result is to decrease the indicated average transverse momentum of the model proposed by Adcock *et al.*[16] by a factor of 0.85. Thus, the conclusions of Adcock *et al.* should be changed to give a mean transverse momentum for their interaction model of 0.5 instead of 0.6 GeV/c. Their model is basically that of Cocconi, Koester, and Perkins[23] (CKP), where $\langle n_\pi\rangle \propto E^{1/4}$.

The doubles to singles ratio in 1 m^2 from Utah previously has agreed poorly[18] with the doubles to singles ratio in 1 m^2 from other works.[8,18] The ratio for the Utah results is obtained by assuming that the inclusive doubles in 1 m^2 consist

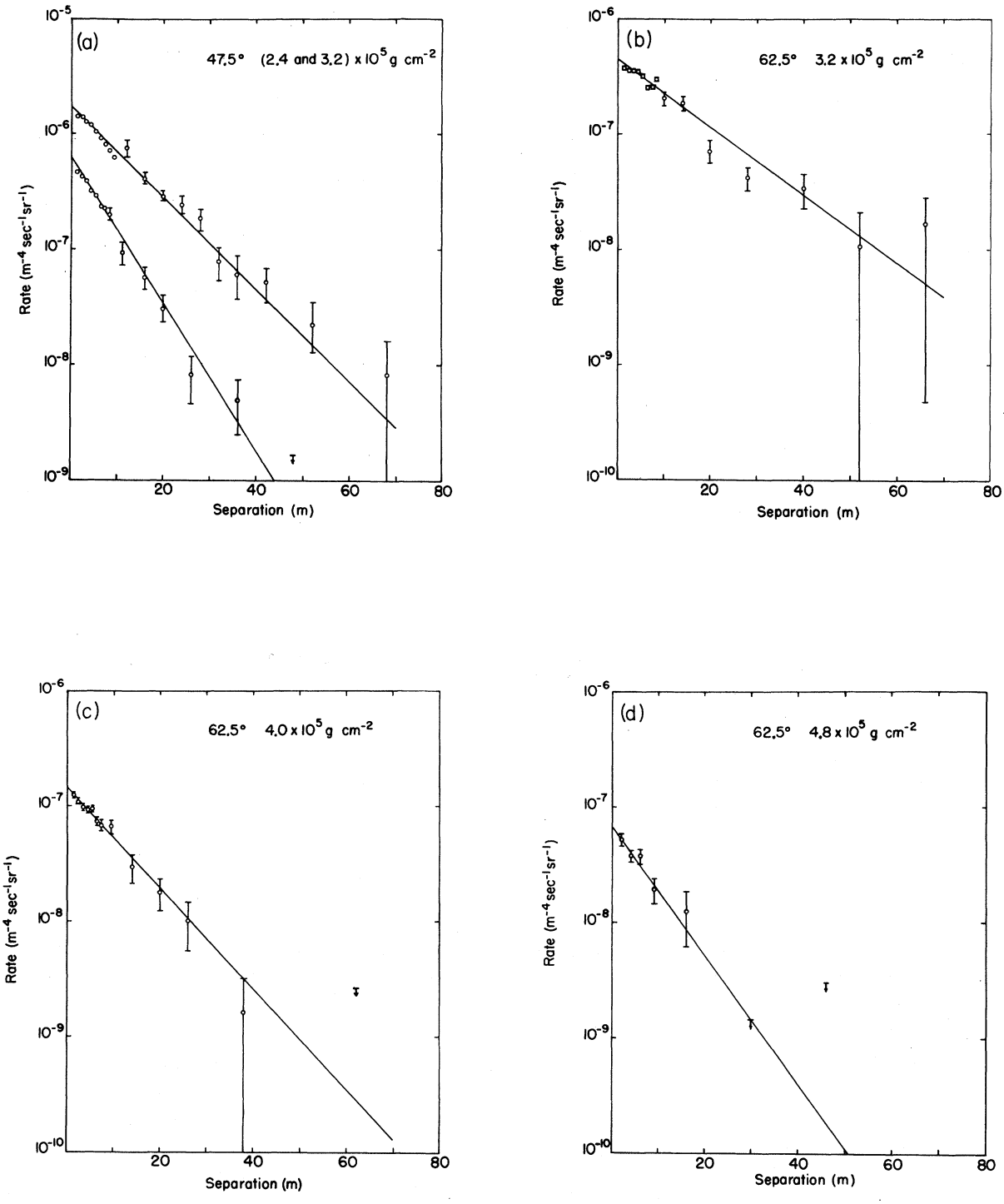

FIG. 4. Decoherence curves of muon showers. Errors are all Gaussian taking into account only the statistical errors. In the case where 0 counts were obtained in a bin the upper bound indicated corresponds to one count. The fits indicated by the lines use Poisson statistics so that any number of counts are handled correctly. Data involving separations from 1.5 to 10.5 m are from the main detector above, while the rest of the data involve the outrigger. In (a) the upper curve is for 2.4×10^5 g/cm^2 and the lower curve is for 3.2×10^5 g/cm^2.

essentially only of exclusive doubles. From this assumption one can use the fit to R_0 and x_0 to find $J(2)$ by a double integral over a 1-m^2 detector.

$$J(2) = \tfrac{1}{2} \int \int R_0 e^{-x/x_0} dA_1 dA_2.$$

The ratio $J(2)/J(1)$ in 1 m^2 in the present work at 45°, 2.4×10^5 g cm^{-2} is $(9.1\pm0.4)\times10^{-4}$. This result is in agreement to within errors with Barrett *et al.*[8] and Krishnaswamy *et al.*[19]

Barrett *et al.*[8] found a falloff length x_0 at 25° and 1.79×10^5 g cm^{-2} of 9 ± 1 m. When the centering function f obtained for the present data is used to extrapolate to the Barrett point the value obtained is 10.1 m. Krishnaswamy *et al.*[19] state that x_0 is approximately 5 m at 22°, 3.375×10^5 g cm^{-2}. The extrapolated value from the present work is 3.1 m.

VI. DISCUSSION

The values obtained for the centering function f differ from those predicted by Adcock *et al.* The exponent β of secθ in the fits of x_0 is greater by approximately 2.5 standard deviations and the exponent γ of E_μ less by 1 standard deviation. However, the correlation terms in the error matrix are large. If γ is fixed at -0.8 in the fit to x_0, χ_r^2 only increases 0.13 to 0.97 and the best value of β is 1.75. Forcing $\gamma=0.8$ and $\beta=1.3$ increases χ_r^2 to 1.74. In addition, the two points which most determine the angular dependence at 47.5° and 62.5°, 3.2×10^5 g cm^{-2} are those most subject to centering errors since the centering for both points is somewhat one-sided. Thus, we regard the different values of β and γ as not being particularly significant.

The values obtained for the exponent δ of the exponent of E_μ for the energy dependence of R_0 also differ from that predicted by Adcock *et al.* Since the depth dependence of the muon intensity, the multiple muon rates, and the decoherence normalization R_0 are all similar, it is likely the value reported here is approximately correct. The discrepancy may be explained by Adcock *et al.* not taking into account fluctuations in the muon energy loss.

These muon decoherence measurements complement other underground muon measurements, such as the intensity of muons and the rates of events with a given number of muons in a detector of a given state.

The contribution of primaries of a given type and energy to the muon intensity is proportional to the mean number $\langle M\rangle$ of muons produced at the depth of observation. Their contribution to the decoherence curve is expected[20] to vary approximately as $\langle M\rangle^2$. For a superposition model, which treats the interactions of heavy primaries as those of a group of free nucleons, the contributions to the muon intensity and the decoherence curve would respectively receive weights A and A^2 for a nucleus of atomic number A at the same energy per nucleon. The higher-multiplicity events produced by heavy and high-energy primaries thus give a relatively more important contribution to the muon decoherence curve than to the muon intensity.

In principle, the information contained in the decoherence curve can be divided into two parts. The integral over area of the decoherence curve is independent of the lateral spread of muons in showers. On the other hand, the shape of the decoherence curve depends on the lateral spread of the showers and is sensitive to the transverse-momentum distribution of the parent mesons. The decoherence-curve shape, therefore, provides a constraint on the transverse momentum distributions used in the calculations of rates of events having a given number of detected muons.

Comparisons of the measured decoherence curves with predictions have been made using a number of models. As mentioned above, adjusting the CKP model of Adcock *et al.* to the present data would give a mean transverse momentum of 0.5 GeV/c in the energy range above about 10 TeV. Goned[21] arrived at the conclusions that Feynman scaling gives a mean transverse momentum 16% higher than does a CKP model to fit the same decoherence curve. Thus, in his calculation, the mean transverse momentum to fit our data would be 0.59 GeV/c.

Bergeson *et al.*,[22] get $\langle p_T\rangle = 0.66\pm0.10$ GeV/c in a scaling model where the transverse-momentum distribution fit to the accelerator data is simply multiplied by 1.5 to fit the decoherence curve. (Their results apply only when the scaling parameter x is greater than 0.01). They also found that in models with $Ed^3\sigma\alpha p_T^{-N} f(p_T/p_{\max})$, there is a somewhat poorer fit than the scaling model just described and that $N=4$ fits better than $N=8$.

ACKNOWLEDGMENTS

The authors are grateful to the many members of the University of Utah Cosmic Ray Group whose united efforts have made the research possible. We express our gratitude to A. Larsen for detector maintenance, to R. Duffin and D. Steck for computer analysis, and to L. Gallegos and B. Keuffel for event scanning. We acknowledge many useful discussions with J. W. Elbert. We thank R. B. Coats for many of the initial concepts and the actual construction of the outrigger detectors.

*Research supported by the National Science Foundation.
†Present address: ESL Inc., Sunnyvale, Ca. 94086.
‡Deceased.
‖Present address: Lawrence Livermore Laboratory, Livermore, Ca. 94550.

[1]H. E. Bergeson *et al.*, in *Proceedings of the Fourteenth International Cosmic Ray Conference* (Max-Planck-Institut fur Extraterrestrische Physik, Munich, Germany, 1975), Vol. 6, p. 2055.
[2]G. H. Lowe *et al.*, Phys. Rev. D 12, 651 (1975).
[3]H. E. Bergeson and C. J. Wolfson, Nucl. Instrum. Methods 51, 47 (1967).
[4]G. L. Cassiday, D. E. Groom, and M. O. Larson, Nucl. Instrum. Methods 107, 509 (1973).
[5]L. K. Hilton, M. L. Morris, and R. O. Stenerson, Nucl. Instrum. Methods 51, 43 (1967).
[6]J. W. Keuffel and J. L. Parker, Nucl. Instrum. Methods 51, 29 (1967).
[7]R. B. Coats *et al.*, J. Phys. A 3, 689 (1970).
[8]P. H. Barrett *et al.*, Rev. Mod. Phys. 24, 133 (1952).
[9]K. H. Davis *et al.*, Phys. Rev. D 4, 607 (1971).
[10]H. E. Bergeson *et al.*, in *Proceedings of the Thirteenth International Cosmic Ray Conference* (University of Denver, Denver, Colo., 1973), Vol. 3, p. 1722.
[11]G. W. Mason, Ph.D. thesis, University of Utah, 1969 (unpublished); M. O. Larson, Ph.D. thesis, University of Utah, 1968 (unpublished).
[12]J. W. Keuffel *et al.*, Acta Phys. Acad. Sci. Hung. 29, Suppl. 4, 183 (1969).
[13]G. L. Cassiday *et al.*, Phys. Rev. Lett. 27, 1964 (1971).
[14]G. W. Carlson, Ph.D. thesis, University of Utah, 1972 (unpublished).
[15]E. R. Martin, Ph.D. thesis, University of Utah, 1968 (unpublished).
[16]C. Adcock *et al.*, J. Phys. A 3, 697 (1970).
[17]G. H. Lowe, University of Utah, Internal Report No. UUCR 138, 1974 (unpublished).
[18]G. H. Lowe, Ph.D. thesis, University of Utah, 1973 (unpublished).
[19]M. R. Krishnaswamy *et al.*, in *Proceedings of the Twelfth International Cosmic Ray Conference* (University of Tasmania, Hobart, Australia, 1971), Vol. 6, p. 2886.
[20]This follows for a Poisson distribution of the number M of muons in showers from primaries of a given type and energy with a decoherence contribution proportional to $M(M-1)$.
[21]A. Goned, Nuovo Cimento 29A, 301 (1975).
[22]H. E. Bergeson *et al.*, Phys. Rev. Lett. 36, 1681 (1975).
[23]G. Cocconi, L. G. Koester, and D. H. Perkins, Lawrence Radiation Laboratory High-Energy Physics Study Seminar No. 28, Part 2 [Report No. VCID-1444, 1961 (unpublished)].